

DOI: 10.1002/cctc.201301015

Dinuclear Zinc–N-Heterocyclic Carbene Complexes for Either the Controlled Ring-Opening Polymerization of Lactide or the Controlled Degradation of Polylactide Under Mild Conditions

Christophe Fliedel,^[a, b] Diogo Vila-Viçosa,^[c] Maria José Calhorda,^{*, [c]} Samuel Dagorne,^{*, [b]} and Teresa Avilés^{*, [a]}

We describe the synthesis of the new Zn–N-heterocyclic carbene (NHC) alkoxide complexes $[(S,C_{NHC})ZnCl(OBn)]_2$ (**5**) and $[(O,C_{NHC})ZnCl(OBn)]_2$ (**6**) for use as ring-opening polymerization (ROP) initiators for lactide polymerization. Complexes **5** and **6** are readily available through an alcoholysis reaction between BnOH and the corresponding Zn–NHC ethyl species $[(S,C_{NHC})ZnCl(Et)]$ (**3**) and $[(O,C_{NHC})ZnCl(Et)]$ (**4**), and species **3** and **4** were obtained from the reaction of $ZnEt_2$ with the *N*-methyl-*N'*-ethylphenylsulfide (**1**·HCl) and *N*-methyl-*N'*-ethylmethylether (**2**·HCl) imidazolium salts, respectively. Both solution and solid-state structural data for Zn benzyloxide species **5** and **6** agree with dimeric structures under the studied conditions (reaction conditions: CH_2Cl_2 or THF, room temperature). A computational analysis of species **3** and **4** supports a dimeric

structure in solution. The Zn^{II} alkoxide species **5** and **6** were found to mediate either the ROP of lactide (in an effective and controlled manner) to produce chain length-controlled polylactide (PLA) or, in the presence of an alcohol source such as MeOH, the controlled degradation of PLA through extensive transesterification reactions to afford methyl lactate as the major product. A thorough DFT computational analysis of the ROP of lactide initiated by complex **5** was performed, which revealed that the operating coordination–insertion mechanism was assisted by the second Zn center, leading to a lower-energy ROP process; this result may be of interest for the future design of well-defined and high-performance metal-based catalysts.

Introduction

Polylactide (PLA), a biodegradable thermoplastic polyester derived from lactic acid, which is a renewable resource, is currently attracting attention for various applications, ranging from biomedical to food packaging and device applications.^[1] It is also considered a promising alternative to petrochemical-based plastics.^[2] Because of rapidly increasing production capacities (150 000 tons/year currently), PLA is predicted to be a high-volume commodity material in the coming years.^[3] PLA is best produced in a controlled manner through the ring-

opening polymerization (ROP) of lactide initiated by molecularly well-defined initiators. Notably, commercial PLA is currently manufactured through the ROP of L-lactide with Sn^{II} octanoate.^[4] Over the past 15 years, intensive research efforts have been directed toward the design and synthesis of ligand-supported metal-based initiators for the stereoselective ROP of *rac*-lactide (*rac*-LA) to access stereoregular PLA with improved properties, and, at present, various metal-based initiators effectively and stereoselectively mediate the ROP of *rac*-LA.^[5,6] The organocatalysts for the ROP of lactide were also developed in the last decade.^[7]

In view of the growing need of PLA, the recycling of PLA through degradation–depolymerization into its starting component (i.e., lactic acid) for reuse and/or for conversion into valuable materials (such as lactate esters, which have applications in cosmetics, fragrances, and food additives) is of current interest.^[8] Although the enzymatic PLA degradation (through hydrolysis) has been established,^[9] the chemical depolymerization of PLA typically requires drastic reaction conditions, which are detrimental to product selectivity and impose a high energy input.^[10] A few representative reports in this area include the following: 1) PLA breakage under harsh acidic or basic conditions (NaOH or HCl),^[11] 2) the use of 4-dimethylaminopyridine for PLA degradation (135 °C, 24 h) via ester cleavage,^[12] and 3) PLA depolymerization through transesterification

[a] Dr. C. Fliedel, Prof. T. Avilés
REQUIMTE, Departamento de Química, Faculdade de Ciências e Tecnologia
Universidade Nova de Lisboa
2829-516 Caparica (Portugal)
E-mail: teresa.aviles@fct.unl.pt

[b] Dr. C. Fliedel, Dr. S. Dagorne
Institut de Chimie de Strasbourg
CNRS-Université de Strasbourg
1 rue Blaise Pascal, 67000 Strasbourg (France)
E-mail: dagorne@unistra.fr

[c] D. Vila-Viçosa, Prof. M. J. Calhorda
Departamento de Química e Bioquímica, CQB
Faculdade de Ciências, Universidade de Lisboa
Campo Grande, Ed. C8, 1749-016 Lisboa (Portugal)
E-mail: mjc@fc.ul.pt

 Supporting information for this article is available on the WWW under <http://dx.doi.org/10.1002/cctc.201301015>.

with Sn^{II} octanoate (120 °C, 24 h).^[13] In contrast, although widely studied for the controlled production of PLA, discrete initiators that can mediate the degradation–depolymerization reaction in a controlled manner and under mild conditions are rare and, to our knowledge, are restricted to the following: 1) group 4 metal complexes bearing salalen-type ligands found to depolymerize PLA at room temperature (through transesterification) in the presence of MeOH^[14] and 2) degradation of PLA with a triazabicyclodecene–alcohol mixture.^[15]

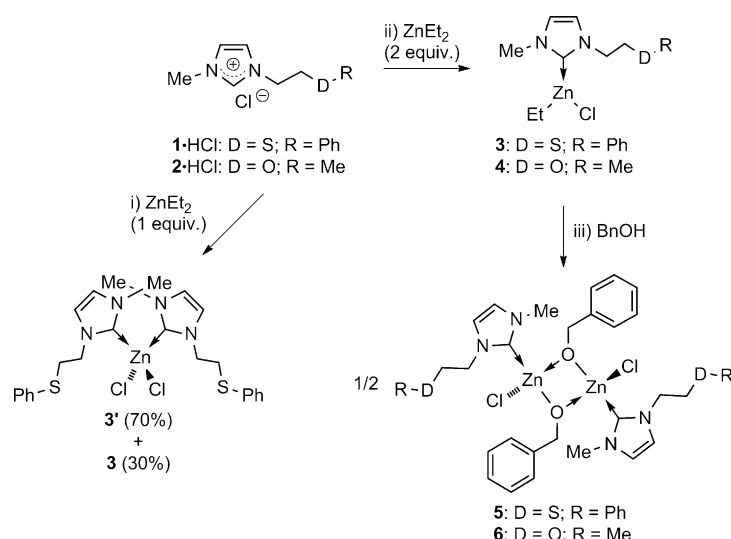
Zn-based alkoxides have been widely investigated as initiators for the ROP of lactide because such derivatives typically demonstrate good to excellent ROP performances.^[16,17] In addition, Zn is cheap, less toxic, and biocompatible, which is important for the subsequent use of the produced PLA in biomedicine. Yet, well-defined Zn alkoxide/amido species frequently decompose in the presence of protic sources, which may significantly hamper their ROP performances and limit their utility.

We are interested in the synthesis of robust N-heterocyclic carbene (NHC)–Zn^{II} alkoxide species for use in the ROP of lactide, a class of species little explored thus far.^[18] The exceptional ligating properties of NHCs should ensure the formation of robust Zn–NHC alkoxide species with improved stability. In addition, such Zn derivatives may be available through straightforward and high-yield syntheses. More specifically, we aimed at the synthesis of new Zn alkoxide complexes of neutral *S*,*C*_{NHC} ligands (in which *S* represents an *N*-thioether functionality) of the type [(*D*,*C*_{NHC})ZnX(OR)] (*X* = halogen, alkyl, aryl, amide; *R* = alkyl, aryl; *D* = neutral donor) for use in the ROP of lactide. The association of such an additional labile soft donor with the NHC ligand may lead to an improvement in the catalytic performance of the system.^[19] As described herein, the synthesized Zn complexes [(*D*,*C*_{NHC})ZnX(OR)] were found to mediate in a controlled manner and under mild conditions either the ROP of lactide (for the production of PLA) or, in the presence of MeOH, the degradation–depolymerization of PLA through transesterification reactions. Theoretical mechanistic investigations of the ROP of lactide initiated by these Zn systems along with the controlled character of both the polymerization and the depolymerization catalysis are also discussed here.

Results and Discussion

Synthesis and characterization

The desired Zn–NHC alkoxide complexes [(*D*,*C*_{NHC})ZnX(OR)] (*D* = *S* or *O*) were prepared through the alcoholysis of the corresponding zinc ethyl complexes [(*D*,*C*_{NHC})ZnClEt], and a prior synthesis of these complexes was thus required. The protonolysis reaction (at the C2 position) of the *N*-methyl-*N*'-ethylphenylsulfide (1-HCl) or *N*-methyl-*N*'-ethylmethylether (2-HCl) imidazolium chlorides, both readily accessible from reported methods,^[19e,20] with 2 equiv. of ZnEt₂ yielded the corresponding



Scheme 1. Synthesis of [(*D*,*C*_{NHC})ZnClEt] (**3** and **4**) and [(*D*,*C*_{NHC})ZnCl(OBn)]₂ (**5** and **6**) (*D* = *S* and *O*, respectively) complexes from the corresponding imidazolium salts. Reaction conditions: i) 1 equiv. of ZnEt₂, THF or CH₂Cl₂, *T* = –40 °C to RT, overnight; ii) 2 equiv. of ZnEt₂, THF or CH₂Cl₂, *T* = –40 °C to RT, overnight; iii) 1 equiv. of BnOH, THF or CH₂Cl₂, *T* = –40 °C to RT, *t* = 2 h.

Zn–NHC adducts [(*S*,*C*_{NHC})ZnCl(Et)] (**3**) and [(*O*,*C*_{NHC})ZnCl(Et)] (**4**), respectively (Scheme 1, route ii). Both species **3** and **4** were isolated in quantitative yield as light brown oils. The use of excess ZnEt₂ (i.e., 2 equiv. in the present case) seems to be required for the quantitative formation of monocarbene Zn–NHC species **3** and **4**, at least in the case of **3**. Thus, the reaction of 1-HCl/ZnEt₂ in a 1:1 ratio resulted in a mixture of the monocarbene adduct **3** and the biscarbene [(*S*,*C*_{NHC})₂ZnCl₂] (**3'**) complex in a 30:70 ratio (Scheme 1, route i), which indicated a fairly basic Zn–Et group in species **3**.

The identity of Zn species **3** and **4** was determined from NMR analysis. Notably, the ¹H NMR spectra for both species demonstrate no imidazolium NCHN resonance but contain signals corresponding to the Zn–Et moiety in the high-field region (≈0.2 (CH₂) and 1.1 (CH₃) ppm). The ¹³C{¹H} NMR spectra of both complexes contain a characteristic *C*_{carbene} resonance at δ 175.65 (**3**) and 175.40 (**4**) ppm. The corresponding Zn alkoxide complexes [(*S*,*C*_{NHC})ZnCl(OBn)]₂ (**5**) and [(*O*,*C*_{NHC})ZnCl(OBn)]₂ (**6**) could be synthesized in quantitative yield through an alcoholysis reaction upon mixing complexes **3** and **4**, respectively, with 1 equiv. of BnOH (reaction conditions: CH₂Cl₂, room temperature). Species **5** and **6** were isolated as colorless solids, which were stable under N₂ in solution for several days and, surprisingly, air stable for hours in the solid state. The ¹H NMR data agree with the proposed formulation, effective *C*_s-symmetric structures, and with no coordination of the (thio)ether moiety to the Zn center. The *C*_{carbene} resonances for complexes **5** and **6** at δ 171.82 and 171.86 ppm, respectively, are in the expected range. In solution, the proposed dimeric forms for the Zn–OBn complexes **5** and **6** were deduced from diffusion-ordered NMR spectroscopy data collected for complex **5**, which yielded a hydrodynamic radius of 6.2 Å and thus a calculated molecular volume of 1010 Å³. The

latter value was compared with the volume of **5** estimated from its molecular dimensions in its dimeric solid-state structure ($14.06 \times 12.57 \times 6.15 = 1087 \text{ \AA}^3$; see below for the molecular structure of **5** determined by X-ray crystallography studies).^[21] The two estimated values are comparable; thus, it is probable that the solid-state dimeric BnO-bridged structure of **5** is retained in solution (reaction conditions: CH_2Cl_2 , room temperature).

The solid-state molecular structures of complexes **5** and **6** were determined by X-ray crystallography studies, and they are depicted in Figure 1. Both complexes crystallized in the $P2_1/c$ space group and consist of centrosymmetric BnO-bridged dimeric structures. In each structure, the Zn metal center adopts a distorted tetrahedral geometry composed of one NHC ligand, one Cl atom, and two OBn moieties forming a Zn_2O_2 core, a common structural feature in Zn aryloxy/alkoxy chemistry.^[18,22] The Zn–C_{carbene} bond lengths—C1–Zn1 = 2.015(4) (**5**) and 2.0255(17) \AA (**6**)—are rather short but remain in the range observed for reported Zn–NHC complexes.^[18,23] Notably, for both complexes, the side-arm donor function (thioether for **5** and ether for **6**) does not interact with the metal center, which, along with the absence of steric hindrance, allows the NHC ligand to coordinate perpendicularly with the Zn_2O_2 core).

DFT^[24] calculations (using Gaussian 09^[25] and PBE0^[26]) were performed on the dimers **3–6**, starting from the experimental X-ray data described above, and on their monomers (**3m–6m**); the DFT-calculated structures of **5m** and **6m** are shown in Figure 2. In the most stable geometry of the monomers **5m** and **6m** (Figure 2), the metal is three coordinated in a planar environment (sum of the three angles is $\approx 360^\circ$). The S or O donors of the NHC side arm are found at a long distance from Zn (i.e., no bond). Tetrahedral coordination around Zn was never observed.

The calculated structures of the dimeric complexes are close to the experimentally determined structures (Figure 1), with C1–Zn1 = 2.040 \AA , Cl1–Zn1 = 2.250 \AA , Zn1–O1 = 2.002 \AA , O1'–Zn1 = 2.004 \AA in **5** and C1–Zn1 = 2.038 \AA , Cl1–Zn1 = 2.252 \AA , O2–Zn1 = 1.998 \AA , and O2'–Zn1 = 2.008 \AA in **6**.

To evaluate the dimer versus monomer preference in solution, the dimerization energy was calculated (as the difference between the energy of the dimer and twice the energy of the monomer). This energy was $-35.3 \text{ kcal mol}^{-1}$ for **5** in the gas phase, which increased to $-61.8 \text{ kcal mol}^{-1}$ in THF and with a higher quality basis set (see the Computational methods section). The corresponding values for **6** were -39.2 and $-62.3 \text{ kcal mol}^{-1}$ in the gas phase and in THF (better basis set), respectively. The dimerization energy was also calculated for complexes **3** and **4** in the gas phase (-11.8 and $-12.3 \text{ kcal mol}^{-1}$, respectively) and in THF (-11.0 and $-7.4 \text{ kcal mol}^{-1}$, respectively). These large monomer versus dimer energy differences thus support the proposal that species **5** and **6** are also dimeric in solution, even in a coordinating solvent such as THF.

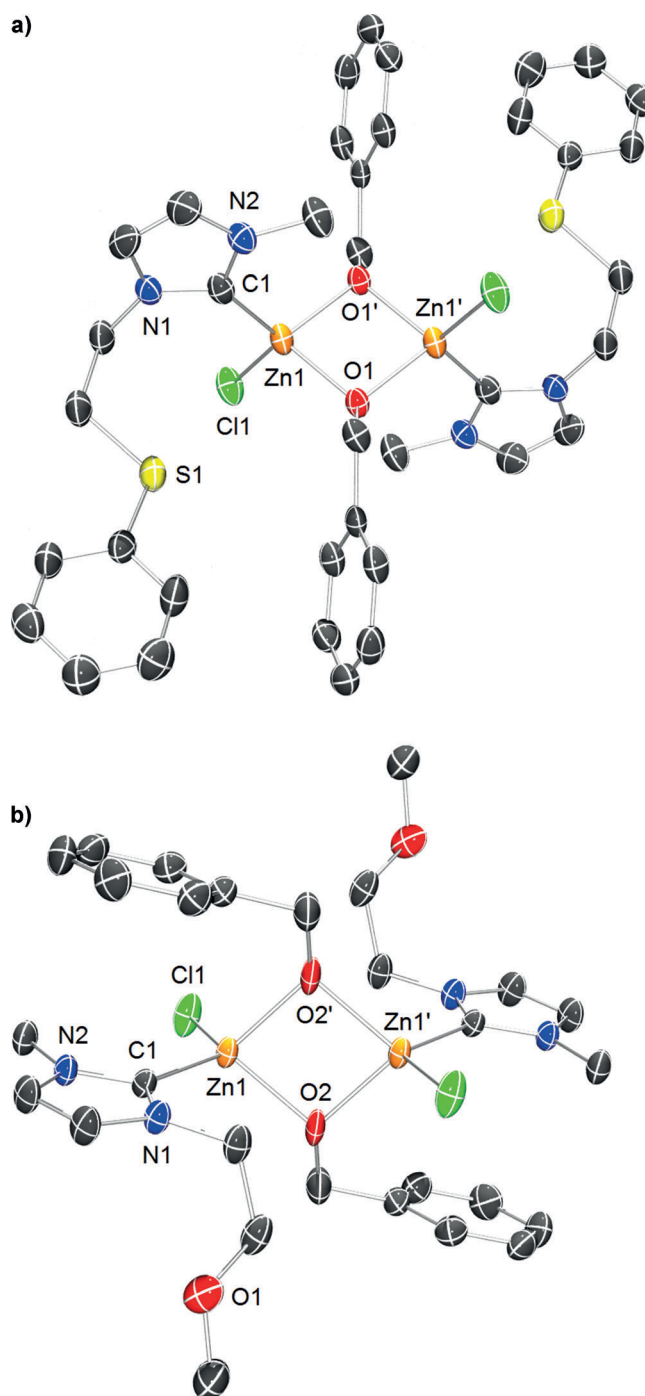


Figure 1. Solid-state molecular structure of a) complex **5** and b) complex **6**. H atoms are omitted for clarity. Selected bond lengths (\AA) for **5**: C1–Zn1 = 2.015(4), Cl1–Zn1 = 2.2412(10), Zn1–O1 = 1.983(2), O1'–Zn1 = 1.994(2); for **6**: C1–Zn1 = 2.0255(17), Cl1–Zn1 = 2.2637(5), O2–Zn1 = 2.0149(13), O2'–Zn1 = 2.0243(14). Bond angles (deg) for **5**: C1–Zn1–Cl1 = 117.47(11), O1–Zn1–O1' = 83.42(10); for **6**: C1–Zn1–Cl1 = 117.19(5), O2–Zn1–O2' = 82.60(6).

ROP of *rac*-LA

The catalytic performances of the synthesized Zn alkoxide complexes (**5** and **6**) were evaluated in the ROP of *rac*-LA for the production of PLA. Both complexes readily polymerize *rac*-LA under mild conditions (100 equiv. of *rac*-LA per Zn, room

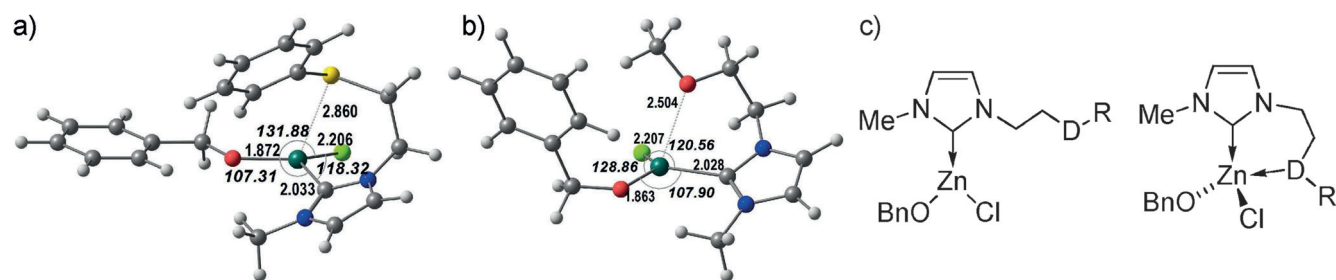


Figure 2. DFT-calculated structures of the mononuclear complexes a) **5 m** and b) **6 m** and c) representation of the envisioned three- or four-coordinated possible structures.

Run	Catalyst	Zn/LA/ BnOH	<i>t</i> [min]	Conversion ^[b] [%]	<i>M_n</i> (corrected) ^[c] [g mol ⁻¹]	<i>M_n</i> (theoretical) ^[d] [g mol ⁻¹]	PDI ^[e]
1	5	1/100/0	90	90	11 486	12 972	1.11
2	5	1/500/0	180	80	10 307	57 656	1.39
3	5	1/300/3	90	89	8969	12 828	1.11
4	5	1/1000/10	120	92	12 474	13 260	1.09
5 ^[f]	5	1/100/0	90	91	10 530	13 116	1.09
6	6	1/100/0	90	84	9672	12 107	1.15

[a] Reaction conditions: CH₂Cl₂, [LA]₀ = 1 M, room temperature; [b] Determined from ¹H NMR analysis; [c] Determined from GPC analysis by using polystyrene standards and applying a correction factor of 0.58;^[28] [d] Calculated according to the conversion (*M_{LA}* = 144.13 g mol⁻¹); [e] Determined from GPC analysis; [f] ROP run in THF.

temperature, 90 min), which afforded narrowly dispersed PLA (1.11 < polydispersity index (PDI) < 1.15) with a good chain length control (see *M_n*(corrected) versus *M_n*(theoretical) in Table 1, runs 1 and 6). The gel permeation chromatography (GPC) analyses confirmed the monomodal mass distribution in agreement with a single-site catalyst; one polymer chain grows per metal center (Figures S1 and S2). All polymerizations mostly gave atactic PLA samples, with racemic linkage probability (*P_r*) ranging from 0.52 to 0.58. The dimer **5**, with a thioether functionality on the NHC side arm, was found to perform best in terms of both control and activity. Compared with earlier reported Zn–NHC alkoxide species,^[18b] initiator **5** demonstrates a comparable ROP activity but enables the production of PLA with narrower polydispersity. However, higher monomer loading led to broader polydispersity and lower ROP control (Table 1, run 2). In the presence of 3 or 10 equiv. of BnOH, complex **5** polymerizes up to 1000 equiv. of the monomer, respectively, in a controlled and immortal manner, which leads to well-defined and narrowly dispersed PLA (PDI = 1.11 and 1.09; Table 1, runs 3 and 4, respectively, and Figure S3). The NMR and matrix-assisted laser desorption time-of-flight (MALDI-TOF) MS data are consistent with the sole presence of the –OBn end group PLA and thus with the noninvolvement of the NHC moiety in the ROP of lactide (Figure S4). This finding suggests that despite an excess of protic source (BnOH), the Zn–NHC bond in these Zn complexes retains its integrity under ROP conditions. The MALDI-TOF spectra also demonstrate low-intensity signals separated by increments of 72 Da,

which suggests residual transesterification reactions as the ROP proceeds (as commonly observed in ligand-supported Zn–OR catalysts).^[27] The linear correlation between the *M_n*(corrected) of the formed PLA and monomer conversion during the polymerization reaction and a nearly constant PDI (Figure 3) are in line with a controlled ROP process. Kinetic studies of the ROP of *rac*-LA initiated by complex **5** agree with a pseudo-first-order reaction rate with respect to monomer: $v = k_{\text{observed}}[\text{LA}]$ (Figure 4).

The ROP of lactide mediated by dimer **5** was investigated through DFT calculations (see the Computational methods section). Several authors have reported DFT calculations on the ROP of lactones to address specific features that could affect it. However, in most studies, the calculation methods have been described briefly, which limits the reliability of the conclusions. In contrast to the present Zn systems, all modeled ROP systems have typically involved monometallic derivatives, such as Al,^[29] Yb,^[30] Ti,^[31] and alkaline and alkaline-earth ROP initiators.^[32] A mechanism involving coordination, nucleophilic attack, and ring-opening reactions (the so-called coordination–insertion mechanism) was determined for the ROP of *rac*-LA initiated by β-diketiminato Mg^{II} species by a thorough DFT computational analysis.^[33] Likewise, the ROP of ε-caprolactone and

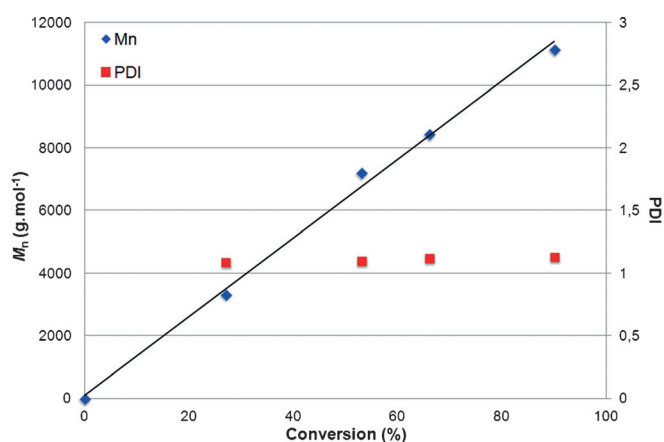


Figure 3. Linear dependence of *M_n* and nearly constant PDI [*M_w*/*M_n*] of PLA versus monomer (LA) conversion with **5** as a catalyst. Reaction conditions: 100 equiv. of *rac*-LA, [LA]₀ = 1 M, CH₂Cl₂, RT.

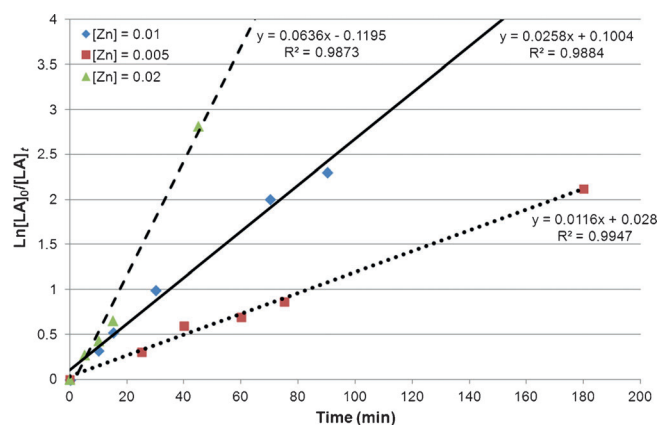


Figure 4. Semilogarithmic plots of *rac*-LA conversion versus time for $[Zn] = 0.005, 0.01, \text{ and } 0.02 \text{ M}$. Reaction conditions: $[Zn]/[LA]_0 = 100, \text{CH}_2\text{Cl}_2, \text{RT}$.

L-lactide initiated by a tridentate phosphorus pincer Zn^{II} species of the type $(\kappa^2\text{-PPP})\text{Zn}\text{-OMe}$ was found to proceed through a coordination–insertion mechanism.^[34] A similar mechanism has been proposed for the ROP of lactide promoted by both $\text{Al}(\text{OH})_3$ and AlMe_2OH .^[35] Although bridging dinuclear metal complexes have been used in this type of polymerization,^[36] only some aspects of the mechanism appear to have been addressed computationally.^[37] Herein, the dimer **5** was used as a catalyst and L-lactide as a substrate (L).

As shown in Figure 1, each Zn^{II} center in complex **5** adopts a slightly distorted tetrahedral coordination with one NHC and one Cl^- ion, which is completed by two nearly symmetrical bridging benzoxide ligands. The pending arms of the NHC containing the SPh group protect the metal and are held in place by weak $\text{C}\text{-H}\cdots\pi$ hydrogen bonds. The approach of the substrate occurs with the formation of weak $\text{C}\text{-H}\cdots\text{Cl}$ and $\text{C}\text{-H}\cdots\text{O}$ hydrogen bonds, leading to an intermediate **A**, which

is considered the reference for the energy profile (0 kcal mol^{-1}). To coordinate the lactide with the metal center, some distortion of the Zn^{II} coordination sphere is required. The easiest way to create a binding position is by moving one of the benzoxides from the bridging to the terminal position, which leaves one of the Zn^{II} centers only three coordinated. The binuclear nature of the catalyst (intermediate **B**) is maintained by the second bridging benzoxide ligand. Schematic representations of these intermediates are shown in Figure 5. In the next step, the benzoxide O atom attacks a carbonyl C atom of the lactide. The two Zn centers are now bridged through the carbonyl O atom of the monomer (intermediate **C**). This fragment rearranges from this $\kappa^1\text{-O}$ coordination mode to a $\kappa^2\text{-O,O}$ mode (intermediate **D**). The final step consists of the cleavage (resulting in ring opening) of the C–O bond of the initial lactide moiety, which yields a benzoxide end-functionalized and ring-opened diester chain (intermediate **E**).

The energy profile of the reaction is shown in Figure 6. The step with the highest barrier is the last step (i.e., from **D** to **E**, involving the opening of six-membered lactide ring), which leads to an overall barrier slightly below 23 kcal mol^{-1} (similar to the value calculated in the gas phase, $\approx 24 \text{ kcal mol}^{-1}$).

The substrate forms a weak $\text{C}\text{-H}\cdots\text{Cl}$ hydrogen bond involving a CH of the lactide ring (2.587 \AA), and the carbonyl O atoms behave as hydrogen bond acceptors toward one CH of the NHC side arm (2.563 \AA) and one CH of the benzoxide ring (2.870 \AA), which barely affects the initial structure of **5** (intermediate **A**). The Zn–Zn bond length remains approximately 2.99 \AA , as in **5**. The substrate approach toward the catalyst (intermediate **A**) is slightly unfavorable in terms of free energy, because it is an associative process but is driven by the large concentration of substrate. A small twisting of the $\kappa^2\text{-O,O}$ benzoxide transforms it into $\kappa^1\text{-O}$ and opens up a coordination position for L, which binds through one carbonyl O atom, affording the new intermediate **B**. The Zn–Zn bond length increases to approximately 3.5 \AA . The energy of intermediate **B** is

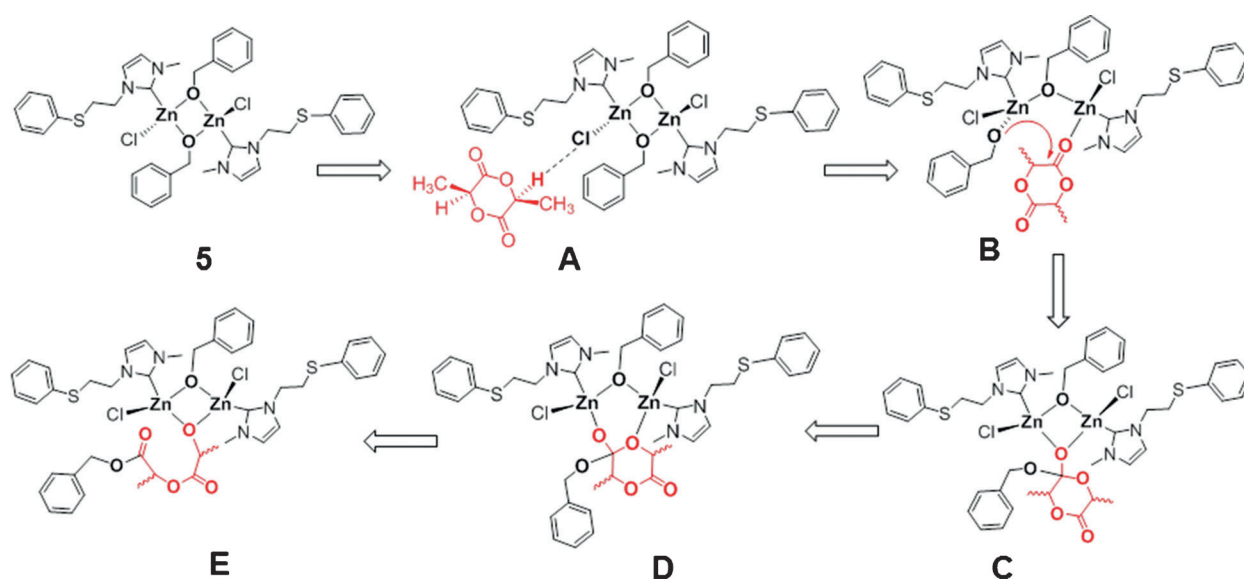


Figure 5. Relevant intermediates in the ROP of L-lactide catalyzed by complex **5**.

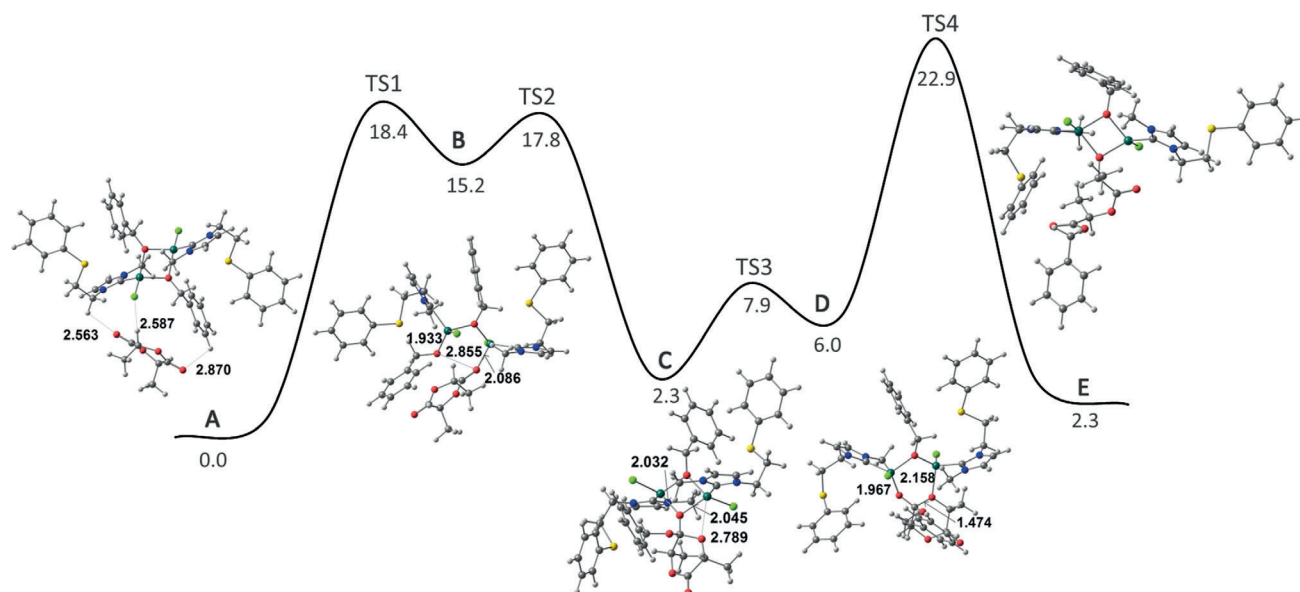


Figure 6. Energy profile for the first cycle in the ROP of lactide catalyzed by complex **5** (Gibbs free energies in kcal mol^{-1}) and structures of the intermediates.

approximately $15.2 \text{ kcal mol}^{-1}$ higher than that of intermediate **A**, with an activation barrier of only approximately $18.4 \text{ kcal mol}^{-1}$. This small value is associated with small rearrangements (no bond cleavage). The small bond length (2.855 \AA) between the benzoxide O atom (charge: -0.695) and the charge-depleted C atom (charge: $+0.711$) of the substrate favors the nucleophilic attack, which leads to the formation of the new C–O bond (intermediate **C**). As a consequence, the benzoxide ligand is no longer bound to Zn and the carbonyl O atom of **L** bridges the two metal atoms, which again move closer (3.063 \AA). Intermediate **C** is much more stable than intermediate **B**, and the activation barrier for the conversion is $2.6 \text{ kcal mol}^{-1}$. This step is relatively similar to that reported using mononuclear Zn^{II} complexes as catalysts,^[34] and the barrier for this specific transformation is smaller in the present binuclear system, emphasizing the assistance provided by the second Zn center, which plays a role in the reaction. In contrast to what has been observed with mononuclear catalysts, the lactide ring opening does not occur immediately, but rather after a rearrangement through binding of one lactide ring O atom to the second Zn atom, which leads to the new intermediate **D** with a small activation barrier ($\approx 5.6 \text{ kcal mol}^{-1}$). This new species has a higher energy ($3.7 \text{ kcal mol}^{-1}$) and a longer Zn–Zn bond length ($\approx 3.4 \text{ \AA}$). The longest C–O bond shown in the structure of **D** (1.474 \AA ; Figure 6) now cleaves, simultaneously with the Zn–O bond, which enables the formation of a C=O bond and gives rise to an acyclic intermediate **E**. As observed previously, the O atom bound to Zn now bridges the two metals. This species compares well with the initial complex **5**, except for the conformations of the SPh arm, which is variable all along the reaction. PLA chain growth is likely to start from intermediate **E**, with a second lactide monomer approaching in a manner similar to that shown in Figure 6. The conformations around Zn are different, and the bridging fragment that undergoes a nucleophilic attack on lactide is much larger.

For this reason, we decided to optimize only the intermediates of the reaction involving the second equivalent of lactide to define the major features of the energy profile. The conformational freedom in intermediates **A**–**E** was neglected. As mentioned above, the SPh arm of the NHC is rather flexible; however, because the steric constraints remained limited, the DFT approach was acceptable. If the second monomer approaches intermediate **E** to form intermediate **A'** and start the second cycle, this limitation becomes more relevant and, to obtain accurate energies, one would need to perform a molecular dynamics study (using either QM or a hybrid QM/MM method), which is beyond the scope of this work. Therefore, the calculated energies should be considered as higher limits.

The second cycle then starts from intermediate **A'** (taken as the energy reference for this cycle) and follows as described in Figure 5, exactly as in the first cycle: the approach of the lactone monomer **L** (**B'**), nucleophilic attack (**C'**), rearrangement (**D'**), and C–O bond opening (**E'**).

The energies of the intermediates are qualitatively similar for the first and the second lactide insertion (Figure 7): intermediates **B**, **C**, and **D** are high-energy species whereas both **E** and **A** are low-energy species. As mentioned previously, we have not taken into account the optimization of side-chain conformations.

The proposed mechanism includes the coordination of L -lactide; the migration of a fragment (here a benzoxide ligand) to the lactide (i.e., a nucleophilic attack), often referred to as the lactide insertion; and the ring-opening reaction. Because we decided not to simplify the structure of catalyst **5** and L -lactide, the overall system is rather large and it is not easy to clearly show the details. The transition states are shown in Figure S5. However, this mechanism covers one complete cycle and cannot thus be well compared with published calculated mechanisms, which usually analyze individual steps. Importantly, the proposed mechanism, which in all steps involves dinu-

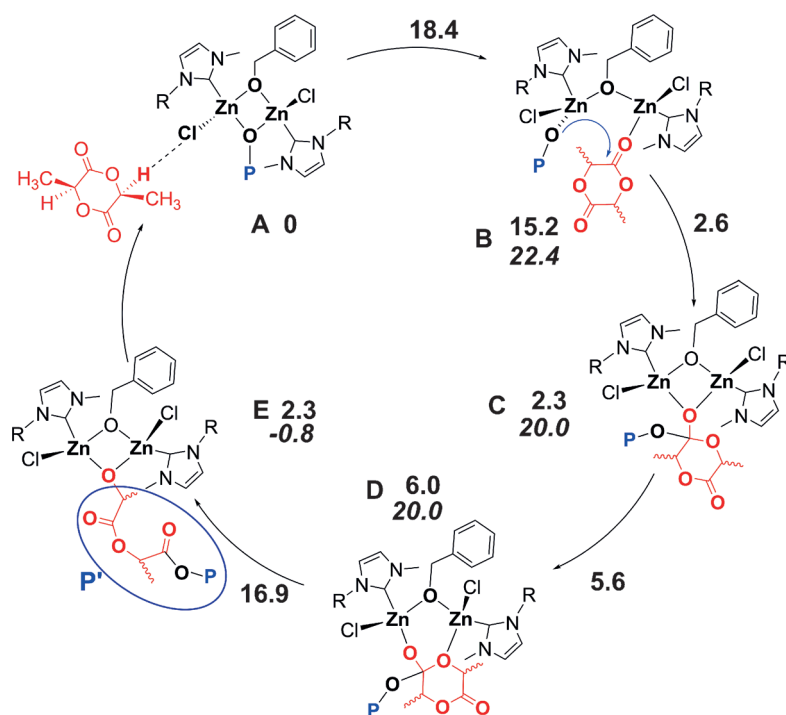


Figure 7. ROP of the first and the second (values in italics) monomer of lactide initiated by complex **5** (Gibbs energies in kcal mol⁻¹), with energies of the intermediates and the activation barriers (first monomer).

clear Zn species, is in line with and further complements the experimental observations on the possibility that dimer **5** is the actual ROP initiator. In addition, the assistance of a second Zn center for a lower-energy ROP process (versus classical mononuclear initiators) has been confirmed and it further highlights that cooperative effects (through, for instance, the use of multinuclear initiators) could be beneficial to the ROP of lactide.

The data on the ROP of lactide initiated by these Zn–NHC benzoxide dimers agree with the finding of one PLA chain growing per Zn center. Two propagating polymer chains are thus expected to grow from the dimeric catalyst; accordingly, we also calculated the energy of the intermediates involved in the formation of the second chain, starting from complex **E**. We assumed that the next monomer approaches on the side of the benzoxide ligand to form intermediate **A2** (Figure S6), and the other growing PLA chain is on the opposite side. The energies of **A2**, **B2**, **C2**, **D2**, and **E2** parallel those shown in Figure 6; of these intermediates, intermediate **B2** is a high-energy species (corresponding to the lactide coordination to one of the Zn centers along with a cleavage of the Zn–OBn–Zn bridge), and intermediates **C2**, **D2**, and **E2** are lower-energy species (Figure S6). This finding suggests a similar path to that calculated for the first growing chain, with the same highest energy barrier for the ring-opening transition state leading to **E2**. In addition, the energies of **5** (dimeric Zn catalyst with two benzoxide ligands), **E** (one benzoxide ligand and one growing PLA chain), and **E2** (two growing PLA chains) are 0, 10.0, and 22.6 kcal mol⁻¹ (Gibbs energies), respectively, which indicates the possibility of a second PLA chain growth as observed ex-

perimentally (actual computed energies would be lower after the optimization of the environment).

PLA degradation

The dinuclear Zn–NHC complexes were not only efficient initiators for the ROP of lactide but also found to mediate the controlled depolymerization of polylactide through extensive transesterification reactions in the presence of MeOH. Two treatments, that is, evaporation to dryness and methanolysis of crude PLA resulting from the ROP of *rac*-LA by species **5** (reaction conditions: catalyst **5**, 100 equiv. of *rac*-LA, CH₂Cl₂, room temperature, *t* = 90 min, 95% conversion), were initially found to yield different materials. Thus, although the ¹H NMR spectrum of the sample that was evaporated to dryness contains

signals corresponding to PLA along with the traces of unreacted *rac*-LA, the ¹H NMR data for methanolized crude PLA [with an excess of cold MeOH (1.2 mL, ≈ 2500 equiv. per Zn), CH₂Cl₂, room temperature, *t* = 30 min] agree with the presence of PLA along with methyl lactate and associated oligomers (methyl lactate/oligomers ratio 1:3; Figure 8). This observation was confirmed by GPC analyses of both the non-MeOH and MeOH

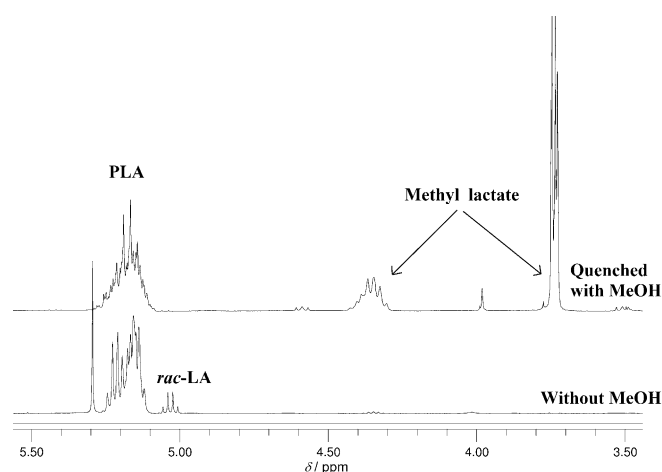
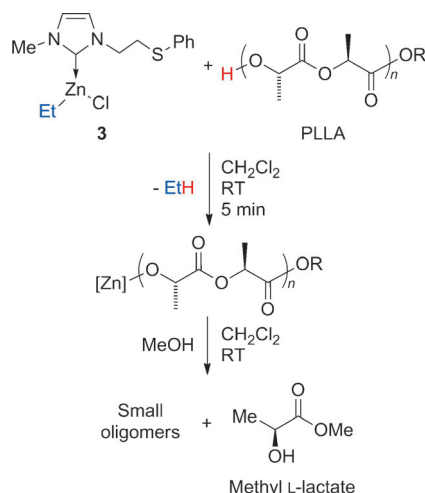


Figure 8. ¹H NMR spectra for the ROP of *rac*-LA initiated by complex **5** without quenching with MeOH (bottom) and after treatment with MeOH (top). Reaction conditions for the lower spectrum: 100 equiv. of *rac*-LA, [LA]₀ = 1 M, 1.17 mL of CH₂Cl₂, RT, *t* = 90 min, polymer isolated by evaporation of the solvent, 95% conversion. Reaction conditions for the upper spectrum: Same conditions, but after 90 min of the reaction time, 1.2 mL of MeOH was added, and after 30 min the mixture was evaporated to dryness.

quenched samples. One peak corresponding to a $M_n(\text{GPC})$ value of 18787 g mol^{-1} was observed for the former, and two peaks corresponding to 5567 and 148 g mol^{-1} for the latter, which was consistent with the formation of smaller oligomers and methyl lactate from the initial PLA (Figures S7 and S8, respectively). Likewise, the treatment of crude PLA (derived from the ROP of *rac*-LA by **5**; $M_n(\text{GPC})=7955 \text{ g mol}^{-1}$) with MeOH (0.5 mL , ≈ 1000 equiv. per Zn center, room temperature, $t=1 \text{ h}$) led to the nearly quantitative formation of methyl lactate along with residual oligomers (methyl lactate/oligomers ratio 10:1), as deduced from GPC (two peaks: M_n values of 140 and 691 g mol^{-1}) and NMR data. On the basis of these preliminary results, the possibility of a Zn-catalyzed mild PLA degradation process proceeding through transesterification with MeOH emerged quickly.

These results prompted us to study the possible use of Zn–NHC complexes described herein for the (controlled) degradation (through transesterification) of poly(L-lactide) (PLLA), the commercial form of PLA. Therefore, a sample of PLLA (200 mg ; $M_n=18410 \text{ g mol}^{-1}$) was first mixed with the NHC–zinc ethyl complex **3** (reaction conditions: CH_2Cl_2 , room temperature, $t=5 \text{ min}$) for the in situ generation of the corresponding NHC–Zn–PLLA species (as deduced from $^1\text{H NMR}$ data) through protonolysis of the Zn–Et bond (Scheme 2). MeOH (100 equiv. per



Scheme 2. PLA degradation starting from an isolated sample of PLLA and mediated by the NHC–zinc ethyl complex **3**.

Zn) was then added, and the degradation of PLA with the concomitant formation of methyl lactate was monitored by using $^1\text{H NMR}$ spectroscopy and GPC. A kinetic study of the depolymerization process could be performed over a period of 24 h . The evolution of the PLLA $M_n(\text{GPC})$ together with the formation of methyl lactate (determined from $^1\text{H NMR}$ data) as a function of time are depicted in Figure 9. A linear decrease in the PLLA M_n along with a linear increase in methyl lactate/smaller oligomers are observed (Figure S9). The GPC analysis of the final product (after a reaction time of 24 h ; Figures S10 and S11) revealed two peaks: one corresponding to an oligomeric material with $M_n(\text{GPC})=2005 \text{ g mol}^{-1}$, and the other as-

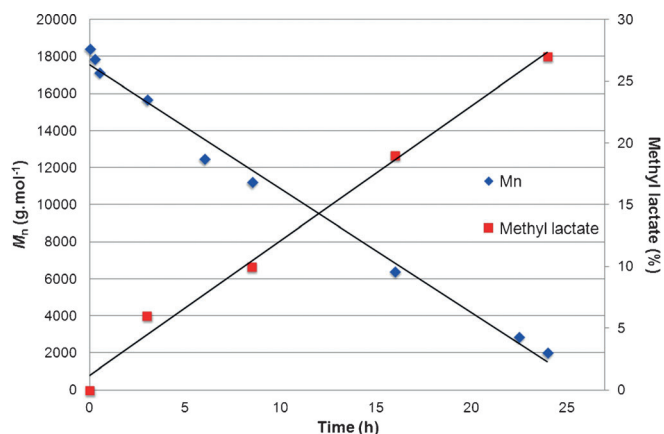


Figure 9. PLLA molecular number (M_n) and formation of methyl lactate (relative to PLLA) versus time in the presence of the 3–MeOH component mixture. Reaction conditions: 200 mg of PLLA with $M_n(\text{GPC})=18410 \text{ g mol}^{-1}$, 5 mg of catalyst **3** (0.014 mmol), 1.43 mL of CH_2Cl_2 , $t=5 \text{ min}$, RT, followed by the addition of $45 \mu\text{L}$ of MeOH (1.4 mmol , 100 equiv. per Zn). t_0 = Time of MeOH addition.

signed to methyl lactate with $M_n(\text{GPC})=145 \text{ g mol}^{-1}$. The MALDI-TOF spectrum of a depolymerization sample (isolated after $t=22.5 \text{ h}$) demonstrated a mass distribution with peaks separated by increments of 72 Da and consistent with the sole presence of MeO end-functionalized lactyl oligomers, which confirmed that the extensive degradation–transesterification of the initial PLA sample had occurred (Figure S12). In an independent NMR control experiment, to probe the stability of the Zn–NHC bond (in complex **5**) in the presence of excess MeOH, species **5** was reacted with 40 equiv. of MeOH (reaction conditions: CH_2Cl_2 , room temperature, $t=2 \text{ h}$), which led to a complete substitution of the Zn–OBn groups by Zn–OMe moieties and, interestingly, only marginal Zn–NHC protonolysis, as deduced from $^1\text{H NMR}$ data. Altogether, the above kinetic and characterization data on the degradation of PLA with a robust Zn–NHC/MeOH component mixture suggest a fairly well controlled process.

Conclusions

These studies confirm that relatively simple dinuclear Zn–N–heterocyclic carbene alkyl/alkoxide complexes can mediate either the ring-opening polymerization of lactide (in an effective and controlled manner) for the production of chain length-controlled polylactide (PLA) or, in the presence of an alcohol source such as MeOH, the controlled depolymerization of PLA through extensive transesterification reactions. Although the polymerization of lactide mediated by Zn-based catalysts has been widely studied, herein we first showed the controlled degradation of PLA under mild conditions to methyl lactate and higher oligomers by well-defined Zn systems, which is a rare instance of a mild catalytic process for the degradation of PLA. We then performed a thorough DFT computational analysis of the polymerization mechanism (of lactide) with these dinuclear Zn-based initiators, which revealed the beneficial effect of a second Zn center for a lower-energy ring-

opening polymerization process; this result may be of interest for the future design of well-defined and high-performance metal-based catalysts.

Experimental Section

General

All experiments were performed under N₂ by using standard Schlenk techniques or in a MBRAUN UNIlab glovebox. Toluene and pentane were collected after passing through drying columns (MBRAUN Solvent Purification Systems) and stored over activated molecular sieves (4 Å) for 24 h in a glovebox before use. THF was distilled over the Na–benzophenone complex and stored over activated molecular sieves (4 Å) for 24 h in a glovebox before use. CH₂Cl₂, CD₂Cl₂, and C₆D₆ were distilled from CaH₂, degassed under a N₂ flow, and stored over activated molecular sieves (4 Å) in a glovebox before use. Anhydrous BnOH (99.8%) was purchased from Aldrich and stored over activated molecular sieves (4 Å) for 24 h in a glovebox before use. All deuterated solvents were obtained from Eurisotop (Groupe CEA, Saclay, France). *rac*-LA (98% purity) was purchased from Aldrich and was sublimed once before use. All other chemicals were purchased from Aldrich and were used as received. The NMR spectra were recorded on Bruker AC 300 or 400 MHz NMR spectrometers with Teflon-valved J. Young NMR tubes at ambient temperature. ¹H and ¹³C chemical shifts were determined by reference to the residual ¹H and ¹³C solvent peaks. The diffusion-ordered NMR spectroscopy experiments were performed with a Bruker 600 MHz NMR spectrometer. Elemental analyses for all compounds were performed at the Service de Microanalyse de la Université de Strasbourg (Strasbourg, France). GPC analyses were performed on a system equipped with a Shimadzu RID10A refractive index detector with HPLC grade THF as an eluant (with molecular masses and PDIs calculated by using polystyrene standards). These were adjusted with appropriate correction factors for the M_n values. MALDI-TOF-MS analyses were performed at the Service de Spectrométrie de Masse de l'Institut de Chimie de Strasbourg and run in a positive mode: samples were prepared by mixing a solution of the polymers in CH₂Cl₂ (0.5 mg 100 mL⁻¹); 2,5-dihydroxybenzoic acid was used as the matrix in a volume ratio of 5:1. Imidazolium salts 1·HCl and 2·HCl were prepared according to literature methods.^[19e,20]

Synthesis of [(D,C_{NHC})ZnClEt] complexes 3 and 4

For **3** (*D*=S): A solution (1 M in hexane) of ZnEt₂ (4.75 mL, 587 mg, 4.75 mmol, 2 equiv.) diluted in CH₂Cl₂ (5 mL) was slowly added to a solution of the imidazolium chloride 1·HCl (605 mg, 2.37 mmol, 1 equiv.) in CH₂Cl₂ (12 mL) at –40 °C. The reaction mixture was then allowed to warm to RT and stirred overnight. The volatiles were then removed under reduced pressure, and the residue was washed twice with pentane (2×10 mL), which yielded a light brown oil. Yield: 93%; ¹H NMR (400 MHz, CD₂Cl₂): δ = 0.18 (q, ³J = 8.0 Hz, 2H; ZnCH₂CH₃), 1.11 (t, ³J = 8.0 Hz, 3H; ZnCH₂CH₃), 3.37 (t, ³J = 6.4 Hz, 2H; NCH₂CH₂S), 3.88 (s, NCH₃, 3H), 4.53 (t, ³J = 6.4 Hz, 2H; NCH₂CH₂S), 6.84 and 6.96 (1H and 1H, AB spin system, ³J = 1.6 Hz; CH=CH), 7.19–7.33 ppm (m, 5H; H_{Ar}); ¹³C{¹H} NMR (100.7 MHz, CD₂Cl₂): δ = 4.62 (br, ZnCH₂CH₃), 11.74 (br, ZnCH₂CH₃), 35.83 (NCH₂CH₂S), 37.95 (NCH₃), 49.78 (NCH₂CH₂S), 122.16 and 126.85 (CH=CH), 129.43 (C phenyl), 129.65 (C phenyl), 129.87 (C phenyl), 135.18 (C *ipso*-phenyl), 175.65 ppm (NCN); elemental analysis calcd (%) for C₁₄H₁₉ClN₂SZn (348.21): C 48.29, H 5.50, N 8.04; found: C 48.41, H 5.34, N 7.90.

For **4** (*D*=O): The same method was followed but with ZnEt₂ (3.74 mL, 461 mg, 3.74 mmol, 2 equiv.) in CH₂Cl₂ (4 mL) and 2·HCl (330 mg, 1.87 mmol, 1 equiv.) in CH₂Cl₂ (10 mL). A light brown oil was obtained. Yield: 90%; ¹H NMR (300 MHz, CD₂Cl₂): δ = 0.16 (q, ³J = 8.1 Hz, 2H; ZnCH₂CH₃), 1.13 (t, ³J = 8.1 Hz, 3H; ZnCH₂CH₃), 3.38 (s br, 3H; OCH₃), 3.72 (t, ³J = 4.8 Hz, 2H; NCH₂CH₂O), 3.90 (s, 3H; NCH₃), 4.43 (t, ³J = 4.8 Hz, 2H; NCH₂CH₂O), 6.94 and 7.07 ppm (1H and 1H, AB spin system, ³J = 1.5 Hz; CH=CH); ¹³C{¹H} NMR (75.5 MHz, CD₂Cl₂): δ = 4.41 (br, ZnCH₂CH₃), 11.53 (br, ZnCH₂CH₃), 37.89 (NCH₃), 50.45 (NCH₂CH₂O), 59.50 (OCH₃), 72.55 (NCH₂CH₂O), 122.02 and 122.58 (CH=CH), 175.40 ppm (NCN); elemental analysis calcd (%) for C₉H₁₇ClN₂OZn (270.08): C 40.02, H 6.34, N 10.37; found: C 39.76, H 6.71, N 10.22.

Synthesis of the [(S,C_{NHC})₂ZnCl₂] complex 3'

The same method as for the synthesis of **3** was followed but with ZnEt₂ (785 μL, 97 mg, 0.785 mmol, 1 equiv.) in CH₂Cl₂ (4 mL) and 1·HCl (200 mg, 0.785 mmol, 1 equiv.) in CH₂Cl₂ (8 mL). No pure sample could be extracted (THF) from the mixture of **3'** and **3** (<5% remaining). Yield: ≈60%; ¹H NMR (300 MHz, CD₂Cl₂): δ = 3.35 (t, ³J = 7.8 Hz, 2H; NCH₂CH₂S), 3.83 (s, 3H; NCH₃), 4.51 (t, ³J = 7.6 Hz, 2H; NCH₂CH₂S), 6.87 and 6.99 (1H and 1H, AB spin system, ³J = 1.8 Hz; CH=CH), 7.17–7.34 ppm (m, 5H; H_{Ar}); ¹³C{¹H} NMR (CD₂Cl₂, 75.5 MHz): δ = 35.17 (NCH₂CH₂S), 37.50 (NCH₃), 49.36 (NCH₂CH₂S), 122.20 and 126.43 (CH=CH), 129.45 (C phenyl), 129.61 (C phenyl), 129.83 (C phenyl), 135.28 (C *ipso*-phenyl), 175.27 ppm (NCN).

Synthesis of [(D,C_{NHC})ZnCl(OBn)]₂ complexes 5 and 6

For **5** (*D*=S): A solution of BnOH (51 μL, 53 mg, 0.49 mmol) in CH₂Cl₂ (5 mL) was added slowly to a solution of complex **3** (170 mg, 0.49 mmol) in CH₂Cl₂ (10 mL) at –40 °C. The reaction mixture was then allowed to warm to RT and stirred for 2 h. The volatiles were then removed under reduced pressure, and the residue was washed twice with pentane (10 mL). Complex **5** was isolated as a white solid after recrystallization from a CH₂Cl₂/pentane solution. Yield: 78%; ¹H NMR (300 MHz, CD₂Cl₂): δ = 3.29 (t, ³J = 8.0 Hz, 2H; NCH₂CH₂S), 3.79 (s, 3H; NCH₃), 4.38 (t, ³J = 8.0 Hz, 2H; NCH₂CH₂S), 4.67 and 4.85 (1H and 1H, AB spin system, ²J = 12.3 Hz; OCH₂Ph), 6.73 and 6.88 (1H and 1H, AB spin system, ³J = 1.8 Hz; CH=CH), 7.04–7.34 ppm (m, 10H; H_{Ar}); ¹³C{¹H} NMR (75.5 MHz, CD₂Cl₂): δ = 34.51 (NCH₂CH₂S), 37.79 (NCH₃), 50.14 (NCH₂CH₂S), 69.04 (OCH₂Ph), 114.78 (C_{Ar}), 121.38 (C_{Ar}), 122.24 (C_{Ar}), 123.05 (C_{Ar}), 126.73 (C_{Ar}), 127.70 (C_{Ar}), 128.23 (C_{Ar}), 129.82 (C_{Ar}), 145.48 (C_{Ar}), 158.64 (C_{Ar}), 171.82 ppm (NCN); elemental analysis calcd (%) for C₃₈H₄₂Cl₂N₄O₂S₂Zn₂ (852.56): C 53.53, H 4.97, N 6.57; found: C 53.37, H 4.79, N 6.54.

For **6** (*D*=O): The same method was followed but with BnOH (58 μL, 60.0 mg, 0.56 mmol) in CH₂Cl₂ (5 mL) and **4** (150 mg, 0.56 mmol) in CH₂Cl₂ (10 mL). Complex **6** was isolated as a white solid after recrystallization from a CH₂Cl₂/pentane solution. Yield: 86%; ¹H NMR (300 MHz, CD₂Cl₂): δ = 3.38 (s br, 3H; OCH₃), 3.72 (t, ³J = 4.8 Hz, 2H; NCH₂CH₂O), 3.90 (s, 3H; NCH₃), 4.43 (t, ³J = 4.8 Hz, 2H; NCH₂CH₂O), 6.94 and 7.07 ppm (1H and 1H, AB spin system, ³J = 1.5 Hz; CH=CH); ¹³C{¹H} NMR (75.5 MHz, CD₂Cl₂): δ = 37.89 (NCH₃), 50.09 (NCH₂CH₂O), 60.10 (OCH₃), 68.55 (OCH₂Ph), 72.74 (NCH₂CH₂O), 114.8 (C phenyl), 121.55 (C phenyl), 122.22 and 122.38 (CH=CH), 129.86 (C phenyl), 154.57 (C phenyl), 171.86 ppm (NCN); elemental analysis calcd (%) for C₂₈H₃₈Cl₂N₄O₄Zn₂ (696.26): C 48.30, H 5.50, N 8.05; found: C 47.91; H 5.32; N 8.20.

Typical polymerization method

In a glovebox, the initiator was charged in a vial equipped with a Teflon tight screw cap and a monomer solution ($[M]_0 = 1 \text{ M}$; THF or CH_2Cl_2) was added with a syringe all at once. The solution was stirred vigorously for an appropriate time and at RT. Upon reaching the desired time, aliquots were taken and analyzed by using ^1H NMR spectroscopy to estimate the conversion. The reaction mixture was exposed to air, and volatiles were removed under vacuum; the resulting solid was then quickly washed several times with MeOH, dried in vacuo until constant weight was achieved, and then analyzed by using ^1H NMR spectroscopy and GPC. In some cases, a MALDI-TOF-MS analysis was performed.

"Immortal" polymerization conditions

A method similar to that described above was used but with the addition of a monomer solution ($[M]_0 = 1 \text{ M}$; CH_2Cl_2) containing the desired amount of BnOH onto complex **5**.

Initial experiments on Zn-mediated PLA degradation

A typical polymerization method was used with the Zn initiator **5**, and the ROP process was performed till complete monomer consumption. The resulting mixture was divided into two equal samples: one was treated as described above for the typical ROP process, and MeOH was added to the other sample and the resulting mixture was stirred at RT until the desired time was reached. In both cases, the mixtures were evaporated in vacuo and subsequently analyzed by using ^1H NMR spectroscopy and GPC.

Kinetic studies of the Zn-mediated degradation of PLLA

In a glovebox, the NHC–zinc ethyl complex **3** was charged in a vial equipped with a Teflon tight screw cap and a PLLA solution (CH_2Cl_2) was added with a syringe all at once. The resulting solution was stirred for 5 min at RT (the disappearance of the Zn–Et signals was monitored by using ^1H NMR spectroscopy). MeOH was then added, and the solution was vigorously stirred for an appropriate time and at RT. Aliquots were taken at regular intervals of time and analyzed to monitor the formation of methyl lactate (by ^1H NMR spectroscopy) and the loss of molecular mass of PLLA (by GPC).

Computational methods

DFT^[24] calculations were performed with the Gaussian 09 software package.^[25] The Perdew–Burke–Ernzerhof functional (PBE0)^[26] was used in all calculations. All geometries were optimized without symmetry constraints and obtained with the Stuttgart/Dresden ECP (SDD) basis set for Zn atoms,^[38] augmented with one polarization function,^[39] and with the 6-31G** basis set^[40] for all the others. The final electronic energies in the gas phase were obtained with the 3-21G basis set^[41] for Zn and the 6-311+G** basis set for all others.^[42] Transition-state optimizations were performed by using the synchronous transit-guided quasi-Newton method,^[43] following extensive searches of the potential energy surface. Frequency calculations were performed to evaluate the nature of optimized geometries. One imaginary frequency was obtained for the transition states and none for the minima. All transition states were confirmed by using the intrinsic reaction coordinate approach. The

X-ray structures of complexes **5** and **6** were used in the calculations of the dimer and to build models of monomers.

All the reported energies (G_{solution}) were calculated by using the following relationship: $G_{\text{solution}} = E_{\text{solution}} + (G_{\text{gas}} - E_{\text{gas}})$. G_{gas} and E_{gas} were obtained from the gas phase calculation, and E_{solution} which is the electronic energy in solution, was obtained by using the integral equation formalism of the polarizable continuum solvation model (IEFPCM)^[44] on the electronic density (SMD).^[45] Three-dimensional representations of calculated structures were obtained with Chemcraft.^[46]

Acknowledgements

We thank Dr. Lydia Brelot and Corinne Bailly for their assistance in the resolution of X-ray structures. We are also grateful to the Fundação para a Ciência e Tecnologia, Portugal, for funding projects (PTDC/QUI-QUI/099873/2008 and PEst-OE/QUI/UI0612/2013) and fellowships (SFRH/BPD/73253/2010 to C.F. and SFRH/BD/81017/2011 to D.V.V.). We also acknowledge the CNRS and the University of Strasbourg for financial support.

Keywords: carbenes · methyl lactate · polylactide degradation · ring-opening polymerization · zinc

- [1] a) E. S. Place, J. H. George, C. K. Williams, M. M. Stevens, *Chem. Soc. Rev.* **2009**, *38*, 1139; b) C. Jérôme, P. Lecomte, *Adv. Drug Delivery Rev.* **2008**, *60*, 1056; c) L. S. Nair, C. T. Laurencin, *Prog. Polym. Sci.* **2007**, *32*, 762; d) M. Vert, *Biomacromolecules* **2005**, *6*, 538; e) A.-C. Albertsson, I. K. Varma, *Biomacromolecules* **2003**, *4*, 1466; f) K. E. Uhrich, S. M. Cannizzaro, R. S. Langer, K. M. Shakesheff, *Chem. Rev.* **1999**, *99*, 3181; g) E. Chiellini, R. Solaro, *Adv. Mater.* **1996**, *8*, 305.
- [2] a) M. Labet, W. Thielemans, *Chem. Soc. Rev.* **2009**, *38*, 3484; b) A. Gandini, *Macromolecules* **2008**, *41*, 9491; c) C. K. Williams, M. A. Hillmyer, *Polym. Rev.* **2008**, *48*, 1; d) A. J. Ragauskas, C. K. Williams, B. H. Davison, G. Britovsek, J. Cairney, C. A. Eckert, W. J. Frederick Jr., J. P. Hallett, D. J. Leak, C. L. Liotta, J. R. Mielenz, R. Murphy, R. Templer, T. Tschaplinski, *Science* **2006**, *311*, 484; e) S. Mecking, *Angew. Chem. Int. Ed.* **2004**, *43*, 1078; *Angew. Chem.* **2004**, *116*, 1096; f) M. S. Lindblad, Y. Liu, A.-C. Albertsson, E. Ranucci, S. Karlsson, *Adv. Polym. Sci.* **2002**, *157*, 139; g) R. E. Drumright, P. R. Gruber, D. E. Henton, *Adv. Mater.* **2000**, *12*, 1841.
- [3] K. Madhavan Nampoothiri, N. R. Nair, R. P. John, *Bioresour. Technol.* **2010**, *101*, 8493.
- [4] a) P. R. Gruber, E. S. Hall, J. J. Kolstad, M. L. Iwen, R. D. Benson, R. L. Borchardt (Cargill Incorporated) US Patent, 5 258 488, **1993**; b) P. R. Gruber, J. J. Kolstad, E. S. Hall, R. S. Eichen Conn, C. M. Ryan (Cargill Incorporated) US Patent, 6 143 863, **2000**.
- [5] For selected reviews, see: a) S. Dagorne, M. Normand, E. Kirillov, J.-F. Carpentier, *Coord. Chem. Rev.* **2013**, *257*, 1869; b) A. Sauer, A. Kapelski, C. Flidel, S. Dagorne, M. Kol, J. Okuda, *Dalton Trans.* **2013**, *42*, 9007; c) A. Arbaoui, C. Redshaw, *Polym. Chem.* **2010**, *1*, 801; d) R. H. Platel, L. M. Hodgson, C. K. Williams, *Polym. Rev.* **2008**, *48*, 11; e) J. Wu, T.-L. Yu, C.-T. Chen, C.-C. Lin, *Coord. Chem. Rev.* **2006**, *250*, 602; f) O. Dechy-Cabaret, B. Martin-Vaca, D. Bourissou, *Chem. Rev.* **2004**, *104*, 6147; g) B. J. O'Keefe, M. A. Hillmyer, W. B. Tolman, *J. Chem. Soc. Dalton Trans.* **2001**, 2215.
- [6] a) A. P. Dove, *Chem. Commun.* **2008**, 6446; b) G. W. Coates, M. A. Hillmyer, *Macromolecules* **2009**, *42*, 7987.
- [7] For specific reviews, see: a) A. P. Dove, *ACS Macro Lett.* **2012**, *1*, 1409; b) M. K. Kiesewetter, E. Ji Shin, J. L. Hedrick, R. M. Waymouth, *Macromolecules* **2010**, *43*, 2093; c) N. E. Kamber, W. Jeong, R. M. Waymouth, R. C. Pratt, B. G. G. Lohmeijer, J. L. Hedrick, *Chem. Rev.* **2007**, *107*, 5813.
- [8] a) C. S. M. Pereira, V. M. T. M. Silva, A. E. Rodrigues, *Green Chem.* **2011**, *13*, 2658; b) R. A. Sheldon, *Green Chem.* **2005**, *7*, 267.
- [9] D. Pirozzi, G. Greco, Jr., *Biotechnol. Prog.* **2006**, *22*, 444.
- [10] Y. Fan, H. Nishida, Y. Shirai, T. Endo, *Green Chem.* **2003**, *5*, 575.

- [11] K. Odelius, A. Höglund, S. Kumar, M. Hakkarainen, A. K. Ghosh, N. Bhatnagar, A.-C. Albertsson, *Biomacromolecules* **2011**, *12*, 1250.
- [12] F. Nederberg, E. F. Connor, T. Glausser, J. L. Hedrick, *Chem. Commun.* **2001**, 2066.
- [13] P. Coszach, J. Willocq (Galactic S.A.) WO 2011/029648A1, **2011**.
- [14] E. L. Whitelaw, M. G. Davidson, M. D. Jones, *Chem. Commun.* **2011**, *47*, 10004.
- [15] F. A. Leibfarth, N. Moreno, A. P. Hawker, J. D. Shand, *J. Polym. Sci. Part A* **2012**, *50*, 4814.
- [16] For recent examples, see: a) N. M. Rezayee, K. A. Gerling, A. L. Rheingold, J. M. Fritsch, *Dalton Trans.* **2013**, *42*, 5573; b) S. Song, X. Zhang, H. Ma, Y. Yang, *Dalton Trans.* **2012**, *41*, 3266; c) V. Poirier, T. Roisnel, J.-F. Carpentier, Y. Sarazin, *Dalton Trans.* **2011**, *40*, 523; d) H. Sun, J. S. Ritch, P. G. Hayes, *Inorg. Chem.* **2011**, *50*, 8063; e) F. Drouin, P. O. Oguadinma, T. J. J. Whitehorn, R. E. Prud'homme, F. Schaper, *Organometallics* **2010**, *29*, 2139; f) D. J. Darenbourg, O. Karroonnirun, *Inorg. Chem.* **2010**, *49*, 2360; g) C. A. Wheaton, P. G. Hayes, *Chem. Commun.* **2010**, *46*, 8404; h) G. Labourdette, D. J. Lee, B. O. Patrick, M. B. Ezhova, P. Mehrkhodavandi, *Organometallics* **2009**, *28*, 1309; i) P. D. Knight, A. J. P. White, C. K. Williams, *Inorg. Chem.* **2008**, *47*, 11711.
- [17] For a review on Zn (Mg and Ca) catalysts for the polymerization of lactide, see: C. A. Wheaton, P. G. Hayes, B. J. Ireland, *Dalton Trans.* **2009**, 4832.
- [18] a) P. L. Arnold, I. J. Casely, Z. R. Turner, R. Bellabarba, R. B. Tooze, *Dalton Trans.* **2009**, 7236; b) T. R. Jensen, C. P. Schaller, M. A. Hillmyer, W. B. Tolman, *J. Organomet. Chem.* **2005**, *690*, 5881; c) T. R. Jensen, L. E. Breyfogle, M. A. Hillmyer, W. B. Tolman, *Chem. Commun.* **2004**, 2504.
- [19] a) C. Fliedel, P. Braunstein, *J. Organomet. Chem.* **2014**, *751*, 286 and references therein; b) M. Bierenstiel, E. D. Cross, *Coord. Chem. Rev.* **2011**, *255*, 574 and references therein; c) C. Fliedel, P. Braunstein, *Organometallics* **2010**, *29*, 5614; d) C. Fliedel, A. Sabbatini, P. Braunstein, *Dalton Trans.* **2010**, *39*, 8820; e) C. Fliedel, G. Schnee, P. Braunstein, *Dalton Trans.* **2009**, 2474.
- [20] L. C. Branco, J. N. Rosa, J. J. Moura Ramos, C. A. M. Afonso, *Chem. Eur. J.* **2002**, *8*, 3671.
- [21] N. Giuseppone, J.-L. Schmitt, L. Allouche, J.-M. Lehn, *Angew. Chem. Int. Ed.* **2008**, *47*, 2235; *Angew. Chem.* **2008**, *120*, 2267.
- [22] a) Y. Huang, W. Wang, C.-C. Lin, M. P. Blake, L. Clark, A. D. Schwarz, P. Mountford, *Dalton Trans.* **2013**, *42*, 9313; b) R. Petrus, P. Sobota, *Dalton Trans.* **2013**, *42*, 13838; c) Y. Wang, W. Zhao, D. Liu, S. Li, X. Liu, D. Cui, X. Chen, *Organometallics* **2012**, *31*, 4182; d) A. Otero, J. Fernández-Baeza, L. F. Sánchez-Barba, J. Tejada, M. Honrado, A. Garcés, A. Lara-Sánchez, A. M. Rodríguez, *Organometallics* **2012**, *31*, 4191; e) C. K. Williams, L. E. Breyfogle, S. K. Choi, W. Nam, V. G. Young Jr., M. A. Hillmyer, W. B. Tolman, *J. Am. Chem. Soc.* **2003**, *125*, 11350; f) M. Cheng, A. B. Attygalle, E. B. Lobkovsky, G. W. Coates, *J. Am. Chem. Soc.* **1999**, *121*, 11583.
- [23] a) A. Rit, T. P. Spaniol, L. Maron, J. Okuda, *Angew. Chem. Int. Ed.* **2013**, *52*, 4664; *Angew. Chem.* **2013**, *125*, 4762; b) G. Schnee, C. Fliedel, T. Avilés, S. Dagorne, *Eur. J. Inorg. Chem.* **2013**, 3699; c) Y. Lee, B. Li, A. H. Hoveyda, *J. Am. Chem. Soc.* **2009**, *131*, 11625; d) G. Anantharaman, K. Elango, *Organometallics* **2007**, *26*, 1089; e) D. Wang, K. Wurst, M. R. Buchmeiser, *J. Organomet. Chem.* **2004**, *689*, 2123; f) A. J. Arduengo III, F. Davidson, R. Krafczyk, W. J. Marshall, M. Tamm, *Organometallics* **1998**, *17*, 3375; g) A. J. Arduengo III, H. V. Rasika Dias, F. Davidson, R. L. Harlow, *J. Organomet. Chem.* **1993**, *462*, 13.
- [24] R. G. Parr, W. Young in *Density Functional Theory of Atoms and Molecules*, Oxford University Press, New York, **1989**.
- [25] Gaussian 09, Revision A.1, M. J. Frisch, G. W. Trucks, H. B. Schlegel, G. E. Scuseria, M. A. Robb, J. R. Cheeseman, G. Scalmani, V. Barone, B. Menucci, G. A. Petersson, H. Nakatsuji, M. Caricato, X. Li, H. P. Hratchian, A. F. Izmaylov, J. Bloino, G. Zheng, J. L. Sonnenberg, M. Hada, M. Ehara, K. Toyota, R. Fukuda, J. Hasegawa, M. Ishida, T. Nakajima, Y. Honda, O. Kitao, H. Nakai, T. Vreven, J. A. Montgomery Jr., J. E. Peralta, F. Ogliaro, M. Bearpark, J. J. Heyd, E. Brothers, K. N. Kudin, V. N. Staroverov, R. Kobayashi, J. Normand, K. Raghavachari, A. Rendell, J. C. Burant, S. S. Lyengar, J. Tomasi, M. Cossi, N. Rega, J. M. Millam, M. Klene, J. E. Knox, J. B. Cross, V. Bakken, C. Adamo, J. Jaramillo, R. Gomperts, R. E. Stratmann, O. Yazyev, A. J. Austin, R. Cammi, C. Pomelli, J. W. Ochterski, R. L. Martin, K. Morokuma, V. G. Zakrzewski, G. A. Voth, P. Salvador, J. J. Dannenberg, S. Dapprich, A. D. Daniels, Ö. Farkas, J. B. Foresman, J. V. Ortiz, J. Cioslowski, D. J. Fox, Gaussian, Inc., Wallingford CT, **2009**.
- [26] J. P. Perdew, K. Burke, M. Ernzerhof, *Phys. Rev. Lett.* **1996**, *77*, 3865.
- [27] a) C. C. Roberts, B. R. Barnett, D. B. Green, J. M. Fritsch, *Organometallics* **2012**, *31*, 4133; b) L. R. Rieth, D. R. Moore, E. B. Lobkovsky, G. W. Coates, *J. Am. Chem. Soc.* **2002**, *124*, 15239.
- [28] a) M. Save, M. Schappacher, A. Soum, *Macromol. Chem. Phys.* **2002**, *203*, 889; b) A. Kowalski, A. Duda, S. Penczek, *Macromolecules* **1998**, *31*, 2114.
- [29] a) I. D. Rosal, R. Poteau, L. Maron, *Dalton Trans.* **2011**, *40*, 11211; b) I. D. Rosal, R. Poteau, L. Maron, *Dalton Trans.* **2011**, *40*, 11228; c) I. S. Vieira, E. L. Whitelaw, M. D. Jones, S. Herres-Pawlis, *Eur. J. Inorg. Chem.* **2013**, 4712.
- [30] B. Liu, T. Roisnel, L. Maron, J.-F. Carpentier, Y. Sarazin, *Chem. Eur. J.* **2013**, *19*, 3986.
- [31] F. Marchetti, G. Pampaloni, C. Pinzino, F. Renili, T. Repo, S. Vuorinen, *Dalton Trans.* **2013**, *42*, 2792.
- [32] a) H.-Y. Chen, L. Mialon, K. A. Abboud, S. A. Miller, *Organometallics* **2012**, *31*, 5252; b) M. Kuzdrowska, L. Annunziata, S. Marks, M. Schmid, C. G. Jaffredo, P. W. Roesky, S. M. Guillaume, L. Maron, *Dalton Trans.* **2013**, *42*, 9352.
- [33] E. L. Marshall, V. C. Gibson, H. S. Rzepa, *J. Am. Chem. Soc.* **2005**, *127*, 6048.
- [34] I. D'Auria, M. Lamberti, M. Mazzeo, S. Milione, G. Roviello, C. Pellicchia, *Chem. Eur. J.* **2012**, *18*, 2349.
- [35] J. L. Eguiburu, M. J. Fernandez-Berridi, F. P. Cossío, J. San Román, *Macromolecules* **1999**, *32*, 8252.
- [36] a) A. F. Douglas, B. O. Patrick, P. Mehrkhodavandi, *Angew. Chem. Int. Ed.* **2008**, *47*, 2290; *Angew. Chem.* **2008**, *120*, 2322; b) A. Pietrangelo, S. C. Knight, A. K. Gupta, L. J. Yao, M. A. Hillmyer, W. B. Tolman, *J. Am. Chem. Soc.* **2010**, *132*, 11649; c) I. Yu, A. Acosta-Ramírez, P. Mehrkhodavandi, *J. Am. Chem. Soc.* **2012**, *134*, 12758; d) K. M. Osten, I. Yu, I. R. Duffy, P. O. Lagaditis, J. C.-C. Yu, C. J. Wallis, P. Mehrkhodavandi, *Dalton Trans.* **2012**, *41*, 8123.
- [37] Y. Sarazin, B. Liu, T. Roisnel, L. Maron, J.-F. Carpentier, *J. Am. Chem. Soc.* **2011**, *133*, 9069.
- [38] M. Dolg, U. Wedig, H. Stoll, H. Preuss, *J. Chem. Phys.* **1987**, *86*, 866.
- [39] A. Höllwarth, M. Böhme, S. Dapprich, A. W. Ehlers, A. Gobbi, V. Jonas, K. F. Köhler, R. Stegmann, A. Veldkamp, G. Frenking, *Chem. Phys. Lett.* **1993**, *208*, 237.
- [40] a) A. D. McLean, G. S. Chandler, *J. Chem. Phys.* **1980**, *72*, 5639; b) K. Raghavachari, J. S. Binkley, R. Seeger, J. A. Pople, *J. Chem. Phys.* **1980**, *72*, 650; c) A. J. H. Wachters, *J. Chem. Phys.* **1970**, *52*, 1033; d) P. J. Hay, *J. Chem. Phys.* **1977**, *66*, 4377; e) K. Raghavachari, G. W. Trucks, *J. Chem. Phys.* **1989**, *91*, 1062; f) R. C. Binning Jr., L. A. Curtiss, *J. Comput. Chem.* **1990**, *11*, 1206; g) M. P. McGrath, L. Radom, *J. Chem. Phys.* **1991**, *94*, 511.
- [41] a) J. S. Binkley, J. A. Pople, W. J. Hehre, *J. Am. Chem. Soc.* **1980**, *102*, 939; b) M. S. Gordon, J. S. Binkley, J. A. Pople, W. J. Pietro, W. J. Hehre, *J. Am. Chem. Soc.* **1982**, *104*, 2797; c) W. J. Pietro, M. M. Francl, W. J. Hehre, D. J. DeFrees, J. A. Pople, J. S. Binkley, *J. Am. Chem. Soc.* **1982**, *104*, 5039.
- [42] T. Clark, J. Chandrasekhar, G. W. Spitznagel, P. v. R. Schleyer, *J. Comput. Chem.* **1983**, *4*, 294.
- [43] a) C. Peng, P. Y. Ayala, H. B. Schlegel, M. J. Frisch, *J. Comput. Chem.* **1996**, *17*, 49; b) C. Peng, H. B. Schlegel, *Isr. J. Chem.* **1993**, *33*, 449.
- [44] G. Scalmani, M. J. Frisch, *Chem. Phys.* **2010**, *132*, 114110.
- [45] A. V. Marenich, C. J. Cramer, D. G. Truhlar, *J. Phys. Chem. B* **2009**, *113*, 6378.
- [46] <http://www.chemcraftprog.com/index.html>.

Received: November 29, 2013

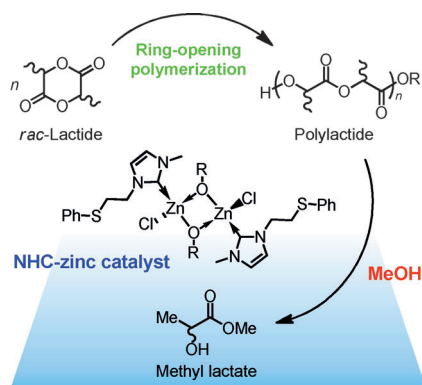
Published online on ■■■■■, 0000

FULL PAPERS

C. Fliedel, D. Vila-Viçosa, M. J. Calhorda,*
S. Dagherne,* T. Avilés*



Dinuclear Zinc–N-Heterocyclic Carbene Complexes for Either the Controlled Ring-Opening Polymerization of Lactide or the Controlled Degradation of Poly lactide Under Mild Conditions



Mild thing: Simple dinuclear zinc–N-heterocyclic carbene (NHC) alkyl/alkoxide complexes mediate, under mild conditions, either the ring-opening polymerization of lactide (in an effective and controlled manner) for the production of chain length-controlled poly lactide or, in the presence of an alcohol source such as MeOH, the controlled depolymerization of poly lactide through extensive transesterification reactions.